

ANNUAL TRANSACTIONS OF THE NORDIC RHEOLOGY SOCIETY, VOL. 6, 1998
FIBRE NETWORK BREAK-UP

Ulf Björkman

Paper Technology, Royal Institute of Technology, Stockholm, Sweden

Abstract

Break-up patterns in fibre networks of different origins have been studied. A number of special instruments have been constructed. A general break-up rule is established. Application to various standard flow geometries shows good agreement. The formation of compressive stress chains in such systems is considered and their presence in fibre floc systems is demonstrated.

INTRODUCTION

In technical processes, fibre networks usually form out of flowing fibre suspensions. Flocs of fibres are normally difficult to disperse completely. Since flows do not to arrest momentarily due to inertia, such dynamically formed flocs normally have time to develop. As a result, many fibre networks consist of closely packed flocs, more or less strongly grown together. This generation process also often makes such networks very heterogeneous, with flocs built up of smaller flocs, which are in turn etc.

The investigated floc networks consist of fibres kept together by cohesive forces, both of mechanical and electrostatic origin. The flocs are compressible *per se* but are suspended in an incompressible low-viscous medium which is relatively loosely bound to the flocs.

Systems of the above type are not uncommon in nature and in technical processes. Even flocculated *non-fibrous* suspensions with relatively freely suspended medium ought to display similar properties. Examples of biological origin can be expected among various natural products, e.g. foods. Examples of inorganic origin may be found in soil systems, and also among larger geological objects. On a micro-level, of course all materials are heterogeneous.

MATERIALS & METHODS

1. Fibre material

Three types of fibre material have been used:

i. Cellulosic fibres in bleached chemical spruce pulp from SödraCell, Mörrum. Concentrations about 1 to 4% by weight, freeness about 20 SR. Unbranched fibres, about 3 mm long and about 22 μm in diameter, giving an aspect ratio of about 140. Fibre density about 1.2 g/ml.

ii. Mycelial fibres of the microbial mould *Penicillium chrysogenum* used in the penicillin process^{1,2,3}. Varying fibre morphology, e.g. degree of branching, about 0.1 to 0.3 mm long and 2 to 4 μm in diameter, giving average aspect ratios of about 25 to 150. Fibre density about 1.1 g/ml.

iii. Black and yellow polyamide fibres (Novalis Fibres, France). Linear fibres with average length of 3 mm and diameter 24 μm , i.e. average aspect ratio 125.

2. Instruments

A number of instruments adapted for the study of coarsely dispersed fibre suspensions were constructed⁴.

i. THE SHEARABLE CUBE

A cubic basin with side length 10 cm in transparent perspex can be sheared to a rhomboid without volume change, Figure 1. The cube is placed in a larger rigid perspex basin. One cube side is fixed and the opposite guided by a milled groove in the bottom of the outer basin, thus allowing it to slide in its own plane. The remaining sides are doubled and expandable through parallel sliding.

The cube is filled with fibre suspension and the outer basin with suspending medium to the same level. The shearing is performed slowly and by hand. Observations can be made from from all sides, also from below.

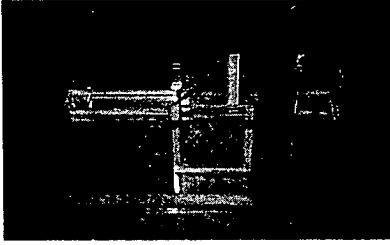


Figure 1. The shearable cube.

ii. THE CHANNEL CIRCUIT

A transparent channel circuit is mounted on a frame to allow inspection from all sides, Figure 2. Its approximate dimensions are; overall length 160 cm, overall width 85 cm, channel height 40 cm and filled volume about 200 l. The central part consists of a tapered section surrounded by two straight sections. The flow is driven by channel-high twin rotors. The flow rate can be varied and reversed by changing the motor speed and direction.

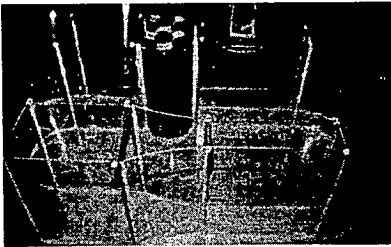


Figure 2. The channel circuit.

iii. THE COUETTE INSTRUMENT

A computerized Couette instrument with independent and programmable cylinder motions was constructed. Gap width 2 cm, bob and cup diameters 10 and 14 cm, cup height 40 cm and filled volume about 3 litres. Bottom treatment of cone-and-plate type, cone height 2 cm. Speed range from creep (also angle positioning) to ± 4000 rpm.

THEORY

The combined plane shearing and extension in Figure 3 is defined by

$$\begin{cases} x = (1 + \epsilon_x)x_0 + \kappa(1 + \epsilon_y)y_0 \\ y = (1 + \epsilon_y)y_0 \end{cases}$$

where $\kappa = \tan \gamma$.

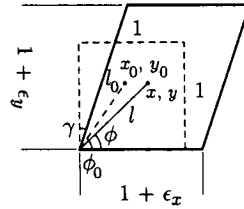


Figure 3. Deformation of a square.

Straightforward trigonometry gives the stretch $\epsilon = (l - l_0)/l_0$ of a line element with initial direction ϕ_0 and final direction ϕ

$$\epsilon = \frac{1}{\sqrt{(\cos \phi - \kappa \sin \phi)^2/\eta_x^2 + \sin^2 \phi/\eta_y^2}} - 1,$$

where $\eta_x = 1 + \epsilon_x$ and $\eta_y = 1 + \epsilon_y$. The largest and smallest stretches occur when $\partial \epsilon / \partial \phi = 0$, which gives

$$\tan 2\phi' = 2\kappa\eta_y^2/[\eta_x^2 - (1 - \kappa^2)\eta_y^2].$$

STRETCHING/COMPRESSION: $\kappa = 0$ gives the principal directions $\phi' = 0$ and 90° .

SHEARING: $\eta_x = \eta_y = 0$ gives $\tan 2\phi' = 2/\kappa$.

RESULTS

i. THE CUBE

The unsheared cube was filled with fibre suspension of about 3.5% by weight and slowly sheared to the left. More or less parallel cracks were found to open up in the direction of the shorter cube diagonal, Figure 4. When the cube was sheared back to its initial state, the cracks closed. The cube was then sheared to the right and new cracks opened up, again more or less parallel to the shortest diagonal. When the cube was finally sheared back to zero, the cracks closed again. This cycle is repeatable and reversible at every point.

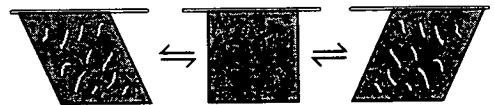


Figure 4. Principal cube cracking results.

ii. THE CHANNEL

Plug cracking patterns were studied in diverging, converging and straight section flows

in pulp suspensions. In expanding flows it was found that cracks tend to align in the flow direction and in contracting flow in the perpendicular direction, Figure 5. In the straight section, the cracks start from both channel walls and extend some distance into the plug, at angles of about 45° against the flow direction. In all sections, the crack directions switched about 90° when the flow direction was reversed.

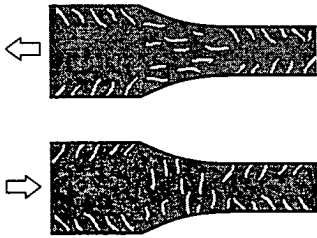


Figure 5. Channel plug flow cracking patterns. Principal results.

iii. THE COUETTE INSTRUMENT

Two principal types of plug cracking patterns were observed, Figure 6; for somewhat lower fibre concentrations (about 1% or so) spiral cracks and for somewhat higher concentrations (say 3%) axial cracks.

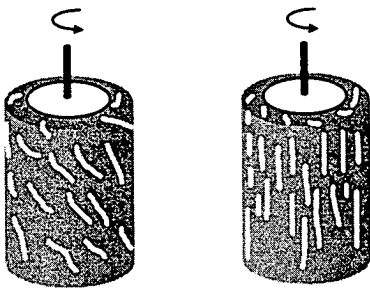


Figure 6. Plug cracking patterns in cylinder viscometers. Principal results. a) At lower concentrations. b) At higher concentrations.

DISCUSSION

1. The cracking rule

The winding cracks in the cube experiment were traced out on transparencies from photographs and the angles were measured with

a graduated arc. Average angles and standard deviations were calculated for different shearing angles γ . On average about 12 cracks per photograph were measured. Figure 7 shows the result together with the theoretical compressive principal direction $\phi' = [\arctan(2/\kappa)]/2$. Fairly large shearings were needed before cracks could be detected safely.

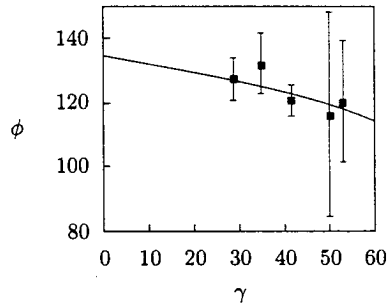


Figure 7. Cube shearings. Points, observed average crack angles ϕ . Shearing angle γ . Line, direction of largest compression.

Within the standard deviation, the average directions coincided with the compressive principal directions.

2. Applications

For the channel, which due to similar stress distribution may also be viewed as a radial section through pipes, the fate of the small material squares in Figure 8 and subsequent application of the cracking rule cover all cases in Figure 5.

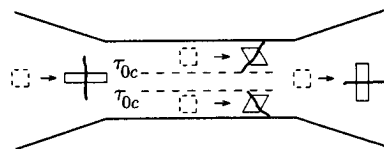


Figure 8. Channel plug flow, plug deformations. Plug cracking strength τ_{0c} .

To understand the Couette results, it necessary to realize that the plug is attached to the cup bottom but, depending on fibre concentration, is more or less unrestricted to slide tangentially against the cylindrical bob and cup surfaces. The tube-formed plug in the

gap therefore experiences tangential shearing stresses over the cup wall layer. The axial section in Figure 9 displays the deformation of a material element.

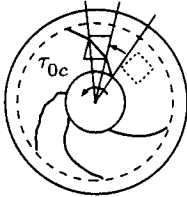


Figure 9. The Couette instrument. Axial view. Tangential plug shearing. Plug cracking strength τ_{0c} .

The cracking rule gives the local crack direction. Connection of crack segments from different radial positions results in the forward bent spirals, which are exponential in the small floc and small shearing limit. Such spirals can be observed at the upper surface in viscometers provided the gap is substantially wider than the floc diameter, compare Figure 12.

Since the plug is fixed to the cup bottom but free at the top surface, it is also subjected to a superposed overall axial torsion. Figure 10 shows the type of axial pattern which the cracking rule predicts when, as in a) the torsional stresses and deformation dominate at somewhat lower fibre concentrations, and as in b) the tangential stresses and deformations dominate at higher concentrations. Intermediate patterns can also often be observed.

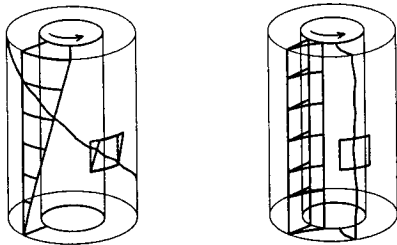


Figure 10. Couette plug flow, plug deformations. a) Torsion, b) Radial shearing.

In the upper surface of a network sedimentation (or rather a plug compaction) in cylin-

ders, a circular cracking pattern can sometimes be observed, indicating axial (telescopic) shearing of the plug.

3. Mechanisms

Most of the water in a normal pulp network can rather easily be squeezed out⁵. The network's own expansive power in directions perpendicular to the superposed compressions is thus insufficient to preserve its volume, i.e. the Poisson ratio $\nu < 0.5$. Consider a volume consisting of a certain amount of fibres in a given volume of water and exclude dewatering. Since both components are incompressible *per se*, the total volume of this element must remain constant under deformation. Let an element of this type be compressed between two parallel large surfaces. The network resistance keeps the plug in close contact with the approaching walls. But, since $\nu < 0.5$ for the network, length deficits between element and network in perpendicular directions are created. These are the prerequisites for the development of finite width cracks.

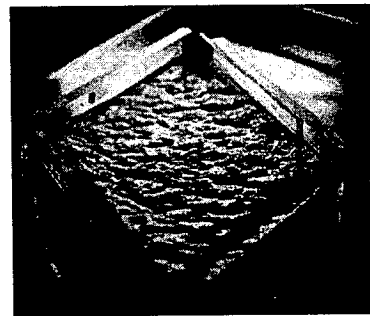


Figure 11. The network cracking experiment. Cube side 10 cm. Paper pulp 3.5%. Cube sheared right.

Oblique views over the free surface in the cube experiment give additional clues, Figure 11. The surface has been pushed up in ridges and valleys. Such directed patterns are not observed in undeformed plugs. The ridges are formed by stress chains composed of stacked flocs. The cracks in Figure 2 are located in the valleys. Cracks of this type

have a tendency to follow weak zones, i.e. between the flocs and, due to the system heterogeneity, along rather winding paths. Analogous free surface behaviour was observed in the channel and Couette plug flows. The forward bowed type of spirals which can be observed in various mixers have the same background, Figure 12. Here a tendency for smaller floc chains to self-organize into larger macro-chains can also be observed.

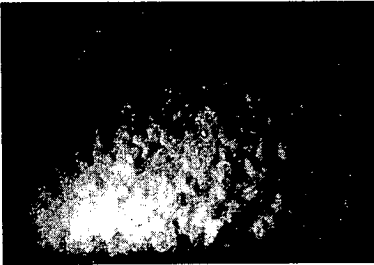


Figure 12. Network spirals in cubical mixed tank. Cube side 1 m. Mixer axis diameter 6 cm. Clockwise rotation 6 rpm.

A stress chain is the result of a mechanism which has focused forces and material along a line (or plane in space). The question of how such stress chains can evolve in loose floc systems, i.e. which are unable to oppose stretchings, can ultimately be brought back to how a displaced floc moves in a surrounding of similar equal sized flocs. Fibre entanglement may play a role but cannot be the complete answer since the flocs can e.g. also roll. An over-simplified linear (Hookean spring) planar example is shown in Figure 13. The central floc is pushed in the positive x -direction whilst being free to move in the y -direction. The elastic potential $E_p(x, y)$ takes the value 0 with the pushed floc at the origin and 1 when it is fully overlapping another floc. The stability lines $\partial E_p / \partial y = 0$ show how the closest neighbouring flocs in *cooperative action* may focus forces. Up to the *pitchfork bifurcation* at $x \approx 0.658$, the resistance to compression from two side flocs outweighs that

of the forward floc. Above $x \approx 0.677$, stability is temporarily lost. More elaborate realistic examples can be built up from such archetypes.

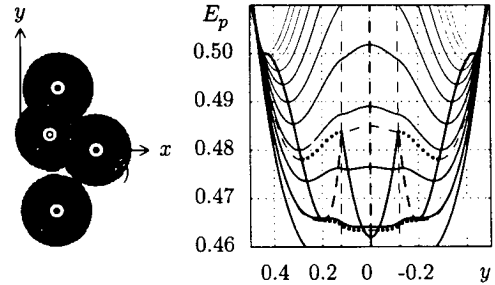


Figure 13. Floc motion in loose Hookean system, $k = 2$. Central floc position (x, y) . $E_p(x, y)$ at $x = \{0.65 : 0.01 : 0.75\}$. Equilibrium lines; unbroken stable, broken labile.

CONCLUSIONS

This cracking and network behaviour is also a key to a better understanding of the flow mechanisms and rheology in such substances^{3,4,6}. Patterns of the demonstrated type can be found in very different environments and may serve as indicator and diagnostic tools.

Acknowledgements

STU, NUTEK, TFR and Carl Tryggers Stiftelse för Vetenskaplig Forskning for financial support.

References

1. Björkman, U. (1986), "Properties and Principles of Mycelial Flow: A Tube Rheometer System for Fermentation Fluids", *Biotechnol. Bioeng.*, **29**, 101-113.
2. Björkman, U. (1986), "Properties and Principles of Mycelial Flow: Experiments with a Tube Rheometer", *Biotechnol. Bioeng.*, **29**, 114-129.
3. Björkman, U. (1991), "Mycelial Flow", monograph, ISBN 91-7170-085-4, KTH, Stockholm.
4. Björkman, U. (1998), "Flow of Flocculated Fibres", report, ISBN 91-7170-178-8, KTH, Stockholm.
5. Steenberg, B. (1984), "Wet Milling: A Model based on Hydrodynamics and Particulate Media Mechanics", *Powder Technology*, **37**, 289-297.
6. Björkman, U. (1997), "Fibre Floc Flow", in Annual Transactions of The Nordic Rheological Society, Ed. A. Friis, Vol. 5, 91-94.